Diffraction at the Tevatron and the LHC *

C. Royon

IRFU/Service de physique des particules
CEA/Saclay, 91191 Gif-sur-Yvette cedex, France

In these lectures, we present and discuss the most recent results on inclusive diffraction at the Tevatron collider and give the prospects at the LHC. We also describe the search for exclusive events at the Tevatron. Of special interest is the exclusive production of Higgs boson and heavy objects (W, top, stop pairs) at the LHC which will require precise measurements and analyses of inclusive and exclusive diffraction to constrain further the gluon density in the pomeron. At the end of these lectures, we describe the projects to install forward detectors at the LHC to fulfil these measurements.

In these lectures, we describe the most recent results on inclusive diffraction at the Tevatron, and especially the search for exclusive events. We finish the lecture by discussing the prospects of diffractive physics at the LHC, and in particular the exclusive diffractive Higgs production. We also describe the diffractive experiments accepted or in project at the LHC: TOTEM, ALFA in ATLAS, and the AFP/FP420 projects.

1. Experimental methods to select diffractive events at the Tevatron and the LHC

In this section, we discuss the different experimental ways to define diffraction at the Tevatron and the LHC.

The Tevatron is a $p\bar{p}$ collider located close to Chicago at Fermilab, USA. It is presently the collider with the highest center-of-mass energy of about 2 TeV. Two main experiments are located around the ring, DØ and CDF. Both collaborations have accumulated a luminosity larger than 3. fb^{-1} with an efficiency larger than 90%.

* Presented at the Summer School on QCD, low x physics, and Diffraction in Copanello, Calabria, Italy, 1-14 July 2007.

As a starting point, we describe the methods to select diffractive events used by the H1 and ZEUS experiments at HERA, DESY, Hamburg in Germany since it is easier. For more details about diffraction at HERA, see the lectures from Bernd Loehr at this Summer school [1].

1.1. The rapidity gap method

HERA was a collider where electrons of 27.6 GeV collided with protons of 920 GeV. A typical event as shown in the upper plot of Fig. 1 is $ep \to eX$ where electron and jets are produced in the final state. We notice that the electron is scattered in the H1 backward detector[1] (in green) whereas some hadronic activity is present in the forward region of the detector (in the LAr calorimeter and in the forward muon detectors). The proton is thus completely destroyed and the interaction leads to jets and proton remnants directly observable in the detector. The fact that much energy is observed in the forward region is due to colour exchange between the scattered jet and the proton remnants. In about 10% of the events, the situation is completely different. Such events appear like the one shown in the bottom plot of Fig. 1. The electron is still present in the backward detector, there is still some hadronic activity (jets) in the LAr calorimeter, but no energy above noise level is deposited in the forward part of the LAr calorimeter or in the forward muon detectors. In other words, there is no color exchange between the proton and the produced jets. As an example, this can be explained if the proton stays intact after the interaction.

This experimental observation leads to the first definition of diffraction: request a rapidity gap (in other words a domain in the forward detectors where no energy is deposited above noise level) in the forward region. For example, the D0 and CDF collaborations at the Tevatron, as well as H1 and ZEUS at HERA, use this method to select diffractive events as we will see it in the following. Let us note that this approach does not insure that the proton stays intact after the interaction, but the proton could be dissociated. The advantage of the rapidity gap method is that it is quite easy to implement and it has a large acceptance in the diffractive kinematical plane.

1.2. Proton tagging

The second experimental method to detect diffractive events is also natural: the idea is to detect directly the intact proton in the final state. The proton loses a small fraction of its energy and is thus scattered at very small

[1] At HERA, the backward (resp. forward) directions are defined as the direction of the outgoing electron (resp. proton).

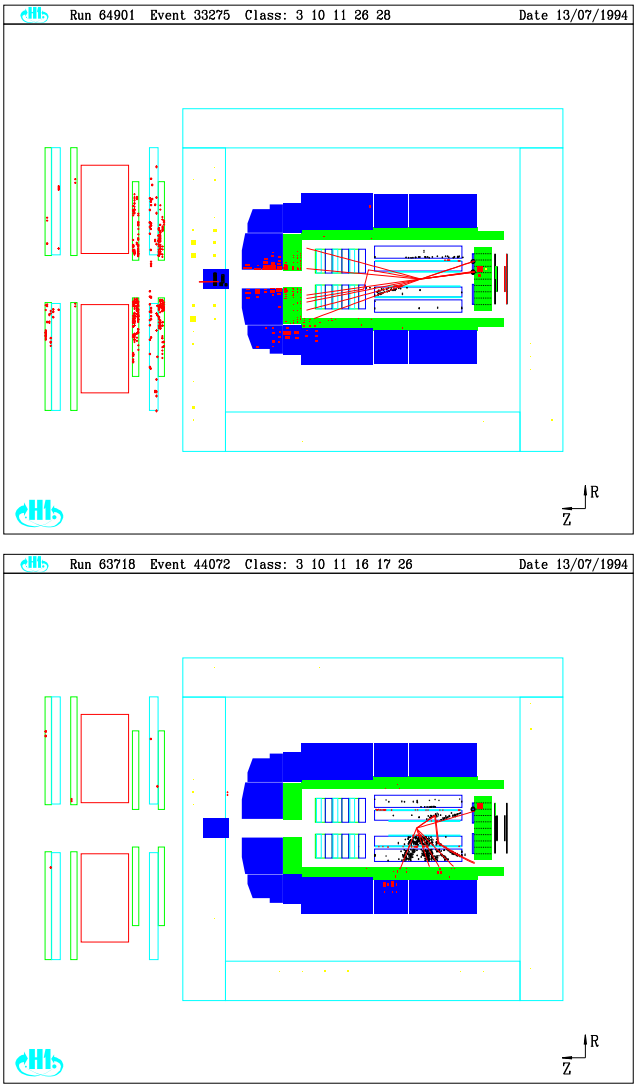

1

Fig. 1. "Usual" and diffractive events in the H1 experiment.

angle with respect to the beam direction. Some special detectors called roman pots can be used to detect the protons close to the beam. The basic idea is simple: the roman pot detectors are located far away from the interaction point and can move close to the beam, when the beam is stable, to detect protons scattered at vary small angles. The inconvenience is that the kinematical reach of those detectors is much smaller than with the rapidity gap method, especially at HERA. On the other hand, the advantage is that it gives a clear signal of diffraction since it measures the diffracted proton directly. This method is also used at the Tevatron and at HERA, and such detectors are or will be installed at the LHC.

A scheme of a roman pot detector as it is used by the H1 or ZEUS experiment is shown in Fig. 2. The beam is the horizontal line at the upper part of the figure. The detector is located in the pot itself and can move closer to the beam when the beam is stable enough (during the injection period, the detectors are protected in the home position). Step motors allow to move the detectors with high precision. A precise knowledge of the detector position is necessary to reconstruct the transverse momentum of the scattered proton and thus the diffractive kinematical variables. The detectors are placed in a secondary vaccuum with respect to the beam one.

1.3. Diffractive kinematical variables

The difference between diffraction at HERA [1] and at the Tevatron is that diffraction can occur not only on either p or $\bar{p}$ side as at HERA, but also on both sides. The former case is called single diffraction whereas the other one double pomeron exchange. In the same way as the kinematical variables x_P and β are defined at HERA, we define $\xi_{1,2}(=x_P$ at HERA) as the proton fractional momentum loss (or as the p or $\bar{p}$ momentum fraction carried by the pomeron), and $\beta_{1,2}$, the fraction of the pomeron momentum carried by the interacting parton. The produced diffractive mass is equal to $M^2 = s\xi_1$ for single diffractive events and to $M^2 = s\xi_1\xi_2$ for double pomeron exchange where $\sqrt{s}$ is the center-of-mass energy [2]. The size of the rapidity gap is of the order of $\Delta\eta \sim \log 1/\xi_{1,2}$.

2. Results on inclusive diffraction from the Tevatron

2.1. Diffractive events at the Tevatron

The DØ and CDF collaborations obtained their first diffractive results using the rapidity gap method which showed that the percentage of single

[2] This formula is valid when the mass of the produced object is larged compared to the proton mass for instance. A more detailed formula is available in Ref. [2] when this is not the case.

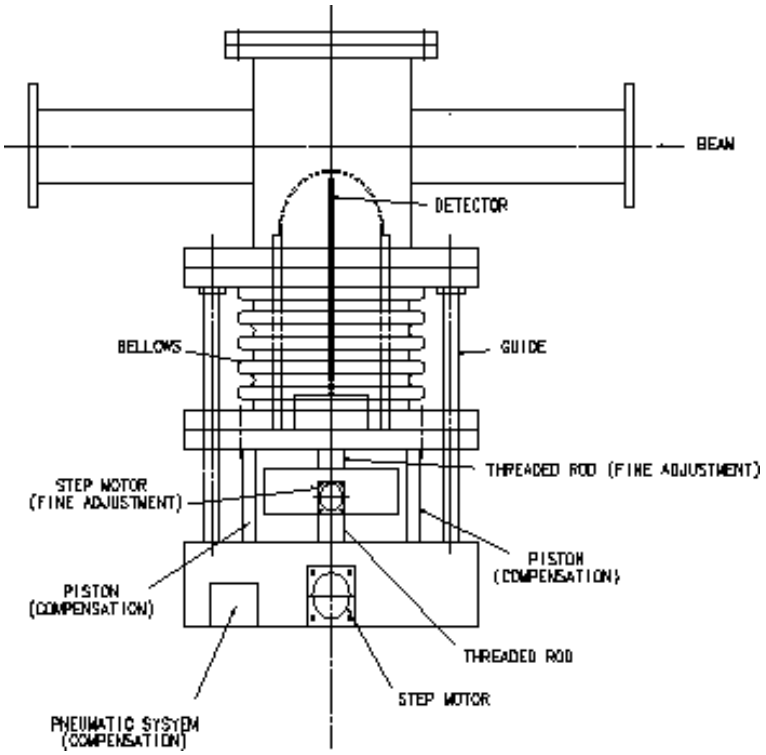

Fig. 2. Scheme of a roman pot detector.

diffractive events was of the order of 1%, and about 0.1% for double pomeron exchanges. This study was made for different experimental observables (Z, jets, J/Ψ...) and was found to be always of the same order of magnitude [3]. Unfortunately, the reconstruction of the kinematical variables is less precise than at HERA if one uses the rapidity gap selection since it suffers from the worse resolution of reconstructing hadronic final states, and this method is not practical to obtain quantitative results.

The other more precise method is to tag directly the p and $\bar{p}$ in the final state, as we mentionned already. The CDF collaboration installed roman pot detectors in the outgoing $\bar{p}$ direction only at the end of Run I [4], whereas the DØ collaboration installed them both in the outgoing p and $\bar{p}$ directions [5]. The DØ (dipole detectors) and CDF roman pots cover the acceptance of t close to 0 and $0.02 < \xi < 0.05$ in the outgoing $\bar{p}$ direction only. In addition, the DØ coverage extends for $0.5 < |t| < 1.5$ GeV^2, and $0.001 < \xi < 0.03$ in both p and $\bar{p}$ directions (quadrupole detectors). The CDF collaboration completed the detectors in the forward region by

adding a miniplug calorimeter on both p and $\bar{p}$ sides allowing a coverage of $3.5 < |\eta| < 5.1$ and some beam showing counters close to beam pipe ($5.5 < |\eta| < 7.5$) allowing to reject non diffractive events.

2.2. From HERA to Tevatron

The starting point for the factorisation studies between HERA and the Tevatron is the measurement of the diffractive structure function F_2^D at HERA [6]. Many different models are used to describe the diffractive structure functions (two-gluon model [7], dipole model [8], or saturation model [9]), which are described in another lecture [1]. Here we will concentrate on the Dokshitzer Gribov Lipatov Altarelli Parisi (DGLAP) [10] fits to F_2^D data. If we assume that the pomeron is made of quarks and gluons [11], it is natural to check whether the DGLAP evolution equations are able to describe the Q^2 evolution of these parton densities. As necessary for DGLAP fits, a form for the input distributions is assumed at a given Q_0^2 and is evolved using the DGLAP evolution equations to a different Q^2, and fitted to the diffractive structure function data at this Q^2 value [1, 12]. The DGLAP QCD fit allows to get the parton distributions in the pomeron as a direct output of the fit. The quark and gluon densities in the pomeron for a Q^2 value of 8.5, 20, 90 and 800 GeV^2 are displayed in Fig. 3 as a function of β. The uncertainty is displayed as a grey shaded area around the central value. We first note that the gluon density is much higher than the quark one, showing that the pomeron is gluon dominated. We also note that the gluon density at high β is poorly constrained which is shown by the larger shaded area [12]. Another fit using another form of input distribution is also displayed in the same figure as a black line [1] which shows even more the bad determination of the gluon density in the pomeron at high β. Let us note that it is possible to constrain further the gluon density in the pomeron by using in addition diffractive jet data in the fit [1, 6]. Even after using jet data, the uncertainty is still large at high β ($\sim$50%) and we will see that this will have some consequences when we will discuss the search for exclusive events at the Tevatron or the LHC.

Once the gluon and quark densities in the pomeron are known, it is easy to make predictions for the Tevatron (or the LHC) if one assumes that the same mechanism is the origin of diffraction in both cases. We assume the same structure of the pomeron at HERA and the Tevatron and we compute as an example the jet production in single diffraction or double pomeron exchange using the parton densities in the pomeron measured at HERA [12]. The interesting point is to see if this simple argument works or not, or in other word if the factorisation property between HERA and the Tevatron — using the same parton distribution functions — holds or not [12].

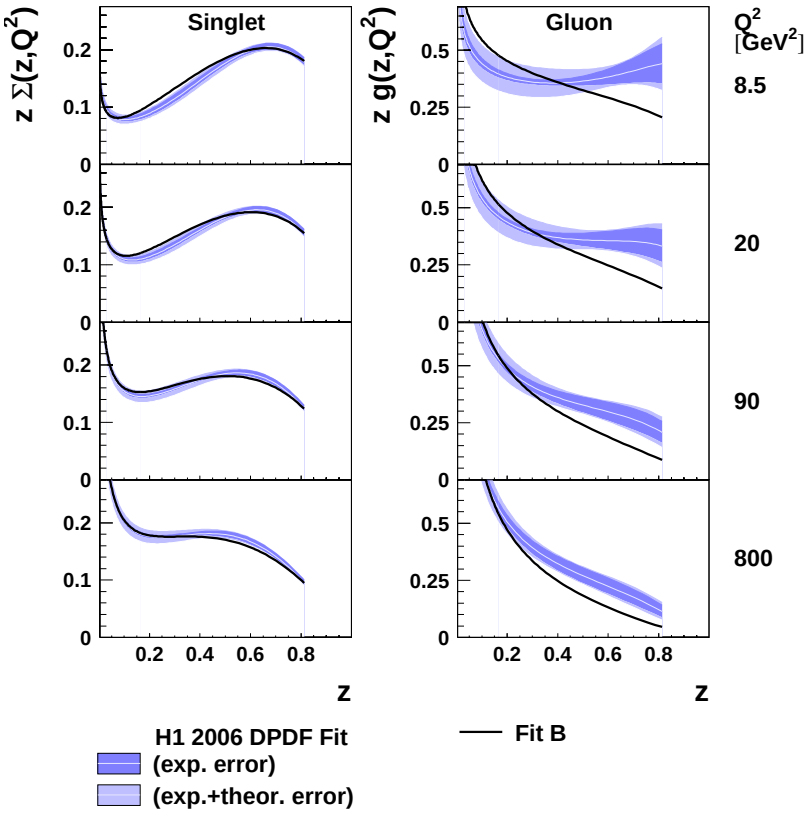

Fig. 3. Extraction of the parton densities in the pomeron using a DGLAP NLO fit (H1 collaboration).

2.3. Factorisation or factorisation breaking at the Tevatron?

The CDF collaboration measured diffractive events at the Tevatron and their characteristics. In general, diffractive events show as expected less QCD radiation: for instance, dijet events are more back-to-back or the difference in azimuthal angles between both jets is more peaked towards π. To make quantitative predictions at the Tevatron and the LHC, it is useful to know if factorisation holds as we mentioned in the previous section. In other words, is it possible to use the parton distributions in the pomeron obtained at HERA to make predictions at the Tevatron, and also further constrain the parton distribution functions in the pomeron since the reach

in the diffractive kinematical plane at the Tevatron and HERA is different? Theoretically, factorisation is not expected to hold between the Tevatron and HERA [13] due to additional pp or $p\bar{p}$ interactions. For instance, some soft gluon exchanges between protons can occur at a longer time scale than the hard interaction and destroy the rapidity gap or the proton does not remain intact after interaction. The factorisation break-up is confirmed by comparing the percentage of diffractive events at HERA and the Tevatron (10% at HERA and about 1% of single diffractive events at the Tevatron) showing already that factorisation does not hold. This introduces the concept of gap survival probability, the probability that there is no soft additional interaction or in other words that the event remains diffractive. We will mention in the following how this concept can be tested directly at the Tevatron for instance.

The first experimental test of factorisation concerns CDF data only. It is interesting to check whether factorisation holds within CDF data alone, or in other words if the β and Q^2 dependence can be factorised out from the ξ one. Fig. 4 shows the percentage of diffractive events as a function of x for different ξ bins and shows the same x-dependence within systematic and statistical uncertainties in all ξ bins supporting the fact that CDF data are consistent with factorisation [14]. The CDF collaboration also studied the x dependence for different Q^2 bins which leads to the same conclusions. This also shows that the Tevatron data do not require additional secondary reggeon trajectories as in H1 [1]. These results show that the soft interactions occuring at a much longer time scale do not depend on the hard scattering. It will be interesting to check if the same conclusions hold at the LHC.

The second step is to check whether factorisation holds or not between Tevatron and HERA data. The measurement of the diffractive structure function is possible directly at the Tevatron. The CDF collaboration measured the ratio of dijet events in single diffractive and non diffractive events, which is directly proportional to the ratio of the diffractive to the "standard" proton structure functions F_2:

$$R(x) = \frac{Rate_{jj}^{SD}(x)}{Rate_{jj}^{ND}(x)} \sim \frac{F_{jj}^{SD}(x)}{F_{jj}^{ND}(x)} \tag{1}$$

The "standard" proton structure function is known from the usual PDFs obtained by the CTEQ or MRST parametrisations. The comparison between the CDF measurement (black points, with systematics errors as shaded area) and the expectation from the H1 QCD fits in full line is shown in Fig. 5 [15]. We notice a discrepancy of a factor 8 to 10 between the data and the predictions from the QCD fit, showing that factorisation does not hold. However,

the difference is compatible within systematic and statistical uncertainties with a constant on a large part of the kinematical plane in β, showing that the survival probability does not seem to be β-dependent within experimental uncertainties. It would be interesting to make these studies again in a wider kinematical domain both at the Tevatron and at the LHC. The understanding of the survival probability and its dependence on the kinematic variables is important to make precise predictions on inclusive diffraction at the LHC.

The other interesting measurement which can be also performed at the Tevatron is the test of factorisation between single diffraction and double pomeron exchange. The results from the CDF collaboration are shown in Fig. 6 [15]. The left plot shows the definition of the two ratios while the right figure shows the comparison between the ratio of double pomeron exchange to single diffraction and the QCD predictions using HERA data in full line. Whereas factorisation was not true for the ratio of single diffraction to non diffractive events, factorisation holds for the ratio of double pomeron exchange to single diffraction! In other words, the price to pay for one gap is the same as the price to pay for two gaps. The survival probability, i.e. the probability not to emit an additional soft gluon after the hard interaction needs to be applied only once to require the existence of a diffractive event, but should not be applied again for double pomeron exchange.

To summarize, factorisation does not hold between HERA and Tevatron as expected because of the long term additional soft exchanges with respect to the the hard interaction. However, experimentally, factorisation holds with CDF data themselves and also between single diffraction and double pomeron exchange which means that the soft exchanges do not depend on the hard scattering, which is somehow natural.

2.4. Possibility of survival probablity measurements at DØ

As we mentionned already, it is very important to test and understand the concept of survival probability. A new measurement can be performed at the Tevatron, in the DØ experiment, which can be decisive to test directly the concept of survival probability at the Tevatron, by looking at the azimuthal distributions of the outgoing proton and antiproton with respect to the beam direction [16].

In Fig. 7, we display the survival probability for three different values of t as a function of the difference in azimuthal angle between the scattered p and $\bar{p}$. The upper black curve represents the case where the t of the p and $\bar{p}$ are similar and close to 0. In that case, only a weak dependence on $\Delta\Phi$ is observed. The conclusion is different for asymmetric cases or cases when t is different from 0: Fig. 7 also shows the result in full red line for the

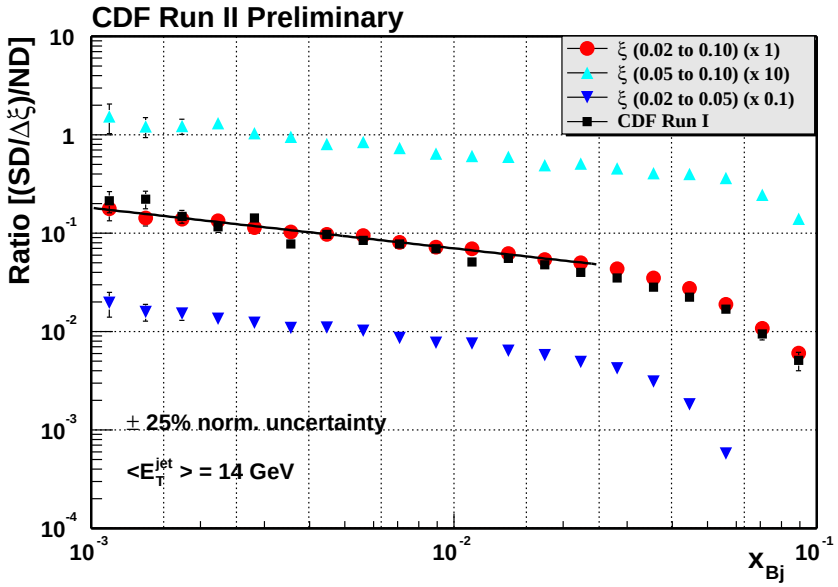

Fig. 4. Test of factorisation within CDF data alone.

asymmetric case ($t_1 = 0.2$, $t_2 = 0.7$ GeV^2), and in full and dashed blue lines for $t_1 = t_2 = 0.7$ GeV^2 for two different models of survival probabilities. We notice that we get a very strong $\Delta\Phi$ dependence of more than one order of magnitude.

The $\Delta\Phi$ dependence can be tested directly using the roman pot detectors at DØ (dipole and quadrupole detectors) and their possibility to measure the azimuthal angles of the p and $\bar{p}$ [16].

The possible measurements can also be compared to expectations using another kind of model to describe diffractive events, namely soft colour interaction [17]. This model assumes that diffraction is not due to a colourless exchange at the hard vertex (called pomeron) but rather to string rearrangement in the final state during hadronisation. In this kind of model, there is a probability (to be determined by the experiment) that there is no string connection, and so no colour exchange, between the partons in the proton and the scattered quark produced during the hard interaction. Since this model does not imply the existence of pomeron, there is no need of a concept like survival probability, and no dependence on $\Delta\Phi$ of diffractive cross sections. The proposed measurement would allow to distinguish between these two drastically different models of diffraction.

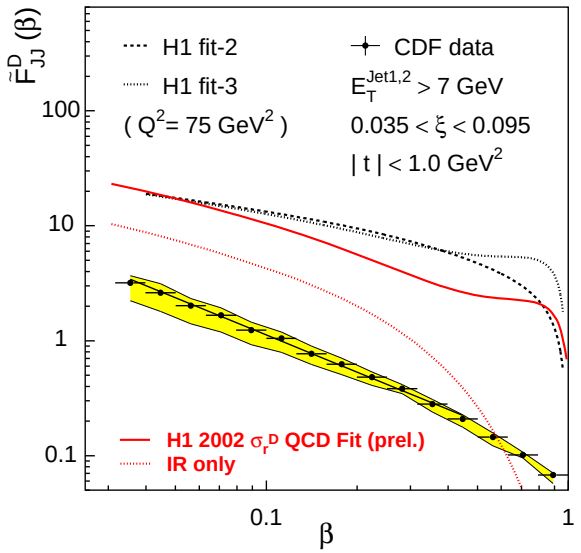

Fig. 5. Comparison between the CDF measurement of diffractive structure function (black points) with the expectation of the H1 QCD fits (red full line).

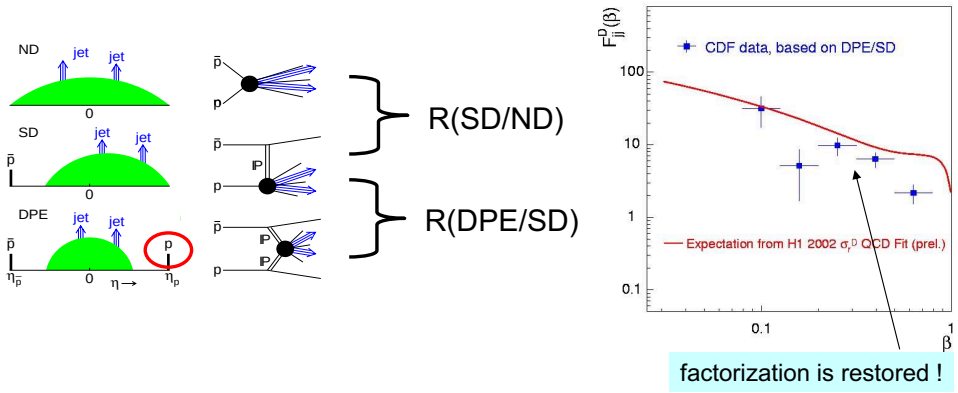

Fig. 6. Restoration of factorisation for the ratio of double pomeron exchange to single diffractive events (CDF Coll.).

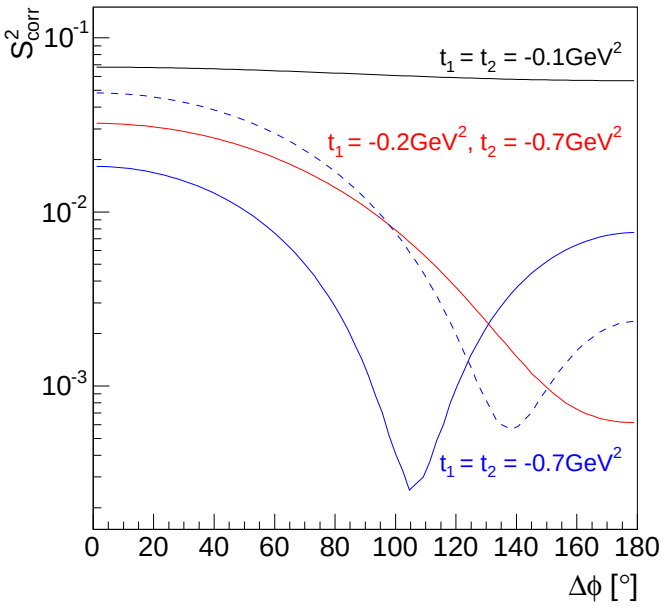

Fig. 7. $\Delta\Phi$ dependence of the survival probability for two different models of survival probability where $\Delta\Phi$ is the difference in azimuthal angle between the scattered p and $\bar{p}$ in the final state, and for three different values of t (see text).

3. Diffractive exclusive event production

3.1. Interest of exclusive events

A schematic view of non diffractive, inclusive double pomeron exchange, exclusive diffractive events at the Tevatron or the LHC is displayed in Fig. 8. The upper left plot shows the "standard" non diffractive events where the Higgs boson, the dijet or diphotons are produced directly by a coupling to the proton and shows proton remnants. The bottom plot displays the standard diffractive double pomeron exchange where the protons remain intact after interaction and the total available energy is used to produce the heavy object (Higgs boson, dijets, diphotons...) and the pomeron remnants. We have so far only discussed this kind of events and their diffractive production using the parton densities measured at HERA. There may be a third class of processes displayed in the upper right figure, namely the exclusive diffractive production. In this kind of events, the full energy is used to produce the heavy object (Higgs boson, dijets, diphotons...) and no energy is lost in pomeron remnants. There is an important kinematical consequence: the

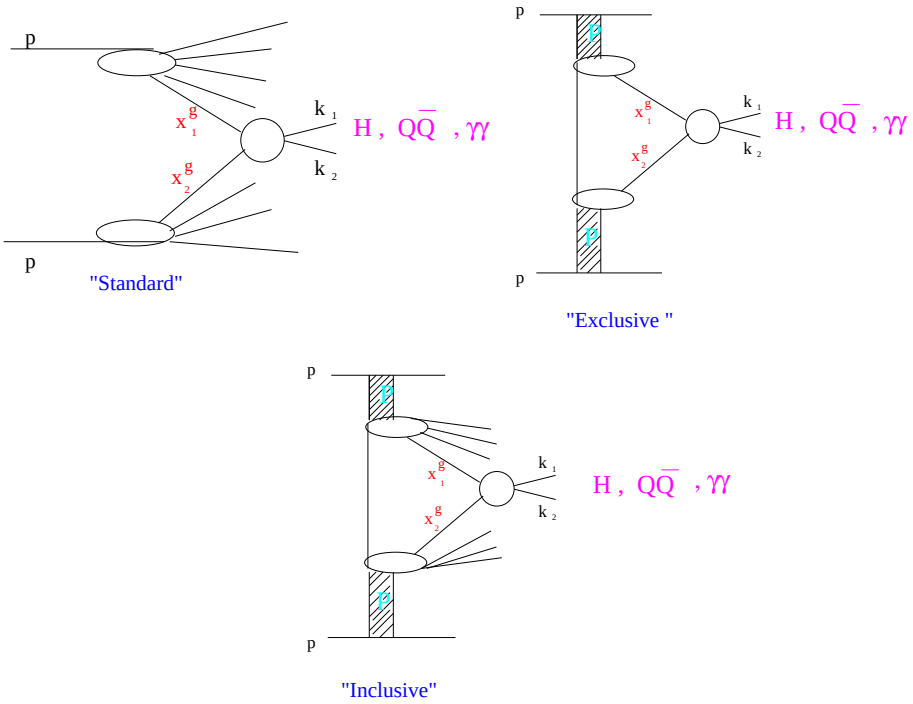

Fig. 8. Scheme of non diffractive, inclusive double pomeron exchange, exclusive diffractive events at the Tevatron or the LHC.

mass of the produced object can be computed using roman pot detectors and tagged protons:

$$M = \sqrt{\xi_1 \xi_2 S}. \tag{2}$$

We see immediately the advantage of those processes: we can benefit from the good roman pot resolution on ξ to get a good resolution on mass. It is then possible to measure the mass and the kinematical properties of the produced object and use this information to increase the signal over background ratio by reducing the mass window of measurement. It is thus important to know if this kind of events exist or not. We will now describe in detail the search for exclusive events in the different channels which is performed by the CDF and D0 collaborations at the Tevatron. In the next section, we will also discuss the impact of the exclusive events on the LHC physics potential.

3.2. Search for exclusive events in χ_c production

One way to look for exclusive events at the Tevatron is to search for the diffractive exclusive production of light particles like the χ mesons. This would give rise to high enough cross sections – contrary to the diffractive exclusive production of heavy mass objects such as Higgs bosons — to check the dynamical mechanisms and the existence of exclusive events. Indeed, exclusive production of χ_c has been studied by the CDF collaboration [18] with an upper limit for the cross section of $\sigma_{exc}(p\bar{p} \to p + J/\psi + \gamma + \bar{p}) \sim 49 \pm 18(stat) \pm 39(sys)$ pb where the χ_c decays into J/Ψ and γ, the J/Ψ decaying itself into two muons. The experimental signature is thus two muons in the final state and an isolated photon, which is a very clear signal. Unfortunately, the cosmics contamination is difficult to compute and this is why the CDF collaboration only quotes an upper limit on the χ_c production cross section. To know if the production is really exclusive, it is important to study the tail of inclusive diffraction which is a direct contamination of the exclusive signal. The tail of inclusive diffraction corresponds to events which show very little energy in the forward direction, or in other words where the pomeron remants carry very little energy. This is why these events can be called quasi-exclusive. In Ref. [2], we found that the contamination of inclusive events into the signal region depends strongly on the assumptions on the gluon distribution in the pomeron at high β — which is very badly known as we mentioned in a previous section. Therefore, this channel is unfortunately not conclusive concerning the existence of exclusive events.

3.3. Search for exclusive events in the diphoton channel

The CDF collaboration also looked for the exclusive production of dilepton and diphoton [19]. Contrary to diphotons, dileptons cannot be produced exclusively via pomeron exchanges since $gg \to \gamma\gamma$ is possible, but $gg \to l^+l^-$ directly is impossible. However, dileptons can be produced via QED processes, and the cross section is perfectly known. The CDF dilepton measurement is $\sigma = 1.6^{+0.5}_{-0.3}(stat) \pm 0.3(syst)$ pb which is found to be in good agreement with QED predictions and shows that the acceptance, efficiencies of the detector are well understood. 3 exclusive diphoton events have been observed by the CDF collaboration leading to a cross section of $\sigma = 0.14^{+0.14}_{-0.04}(stat) \pm 0.03(syst)$ pb compatible with the expectations for exclusive diphoton production at the Tevatron. Unfortunately, the number of events is very small and the cosmics contamination uncertain. The conclusions about the existence of exclusive events are thus uncertain. This channel will be however very important for the LHC where the expected exclusive cross section is much higher.

3.4. Search for exclusive events using the dijet mass fraction at the Tevatron

The CDF collaboration measured the so-called dijet mass fraction in dijet events — the ratio of the mass carried by the two jets produced in the event divided by the total diffractive mass — when the antiproton is tagged in the roman pot detectors and when there is a rapidity gap on the proton side to ensure that the event corresponds to a double pomeron exchange. The CDF collaboration measured this quantity for different jet p_T cuts [20]. We compare this measurement to the expectation coming from the structure of the pomeron coming from HERA. For this sake, one takes the gluon and quark densities in the pomeron measured at HERA as described in Ref. [1, 12] and the factorisation breaking between HERA and the Tevatron is assumed to come only through the gap survival probability (0.1 at the Tevatron).

In Fig. 9, we recall the gluon and quark densities in the pomeron measured at HERA. The gluon density at high β is not well constrained from the QCD fits performed at HERA. To study this uncertainty, we multiply the gluon distribution by the factor $(1-\beta)^\nu$ as shown in Fig. 9. The ν parameter varies between -1 and 1. For $\nu = -1$, the gluon density in the pomeron is enhanced at high β whereas it is damped when ν =1. QCD fits to the H1 data lead to the uncertainty on the ν parameter $\nu = 0.0 \pm 0.5$ [12].

The comparison between the CDF data for a jet p_T cut of 10 GeV as an example and the predictions from inclusive diffraction is given in Fig. 10, left. We also give in the same figure the effects of changing the gluon density at high β (by changing the value of the ν parameter) and we note that inclusive diffraction is not able to describe the CDF data at high dijet mass fraction, even after increasing the gluon density in the pomeron at high β (multiplying it by $1/(1-\beta)$), where exclusive events are expected to appear [21]. The conclusion remains unchanged when jets with $p_T > 25$ GeV are considered [21].

Adding exclusive events to the distribution of the dijet mass fraction leads to a good description of data [21] as shown in Fig. 10, right, where we superimpose the predictions from inclusive and exclusive diffraction. This study does not prove that exclusive events exist but shows that some additional component with respect to inclusive diffraction is needed to explain CDF data. Adding exclusive diffraction allows to explain the CDF measurement. To be sure of the existence of exclusive events, the observation will have to be done in different channels and the different cross sections to be compared with theoretical expectations. In Ref. [21], the CDF data were also compared to the soft colour interaction models [17]. While the need for exclusive events is less obvious for this model, especially at high jet p_T, the jet rapidity distribution measured by the CDF collaboration is

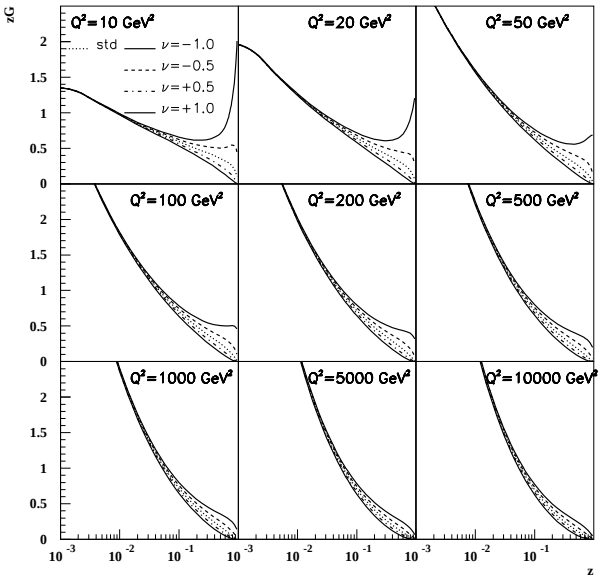

Fig. 9. Uncertainty of the gluon density at high β (here $\beta \equiv z$). The gluon density is multiplied by the factor $(1-\beta)^{\nu}$ where ν=-1., -0.5, 0.5, 1. The default value $\nu = 0$ is the gluon density in the pomeron determined directly by a fit to the H1 F_2^D data with an uncertainty of about 0.5.

badly reproduced. This is due to the fact that, in the SCI model, there is a large difference between requesting an intact proton in the final state and a rapidity gap.

Another interesting observable in the dijet channel is to look at the fraction of b jets as a function of the dijet mass fraction. In exclusive events, the b jets are suppressed because of the $J_Z = 0$ selection rule [22], and it is expected that the fraction of b jets in the diffractive dijet sample diminishes as a function of the dijet mass fraction. The results from the CDF collaboration are given in Fig. 11 [20]. We see a tendency of the b/c jet fraction in data to go down as a function of the dijet mass ratio but the statistics is still low.

Another way to look for exclusive events is to study the correlation between the gap size measured in both p and $\bar{p}$ directions and the value of $\log 1/\xi$ measured using roman pot detectors [23]. The gap size between the pomeron remnant and the protons detected in roman pot detector is of the order of $\log 1/\xi$ for usual diffractive events while exclusive events show a

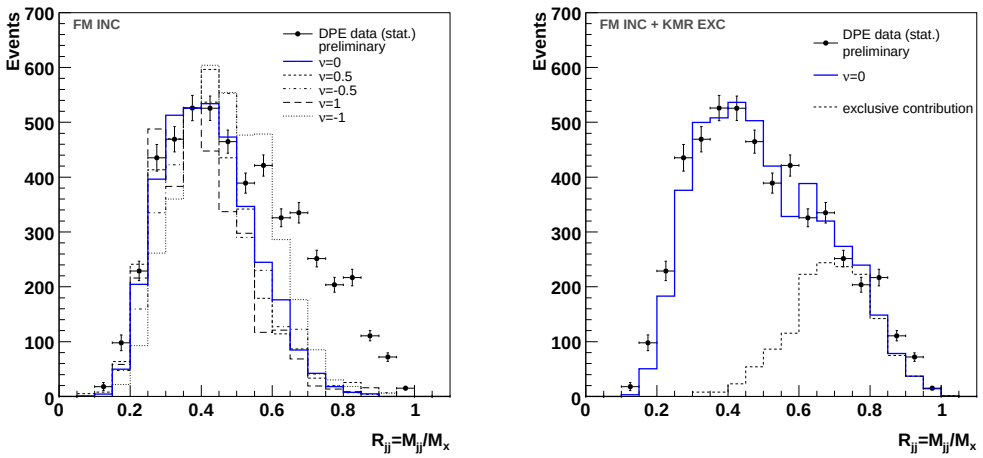

Fig. 10. Left: Dijet mass fraction measured by the CDF collaboration compared to the prediction from inclusive diffraction based on the parton densities in the pomeron measured at HERA. The gluon density in the pomeron at high β was modified by varying the parameter ν. Right: Dijet mass fraction measured by the CDF collaboration compared to the prediction adding the contributions from inclusive and exclusive diffraction.

larger rapidity gap since the gap occurs between the jets and the proton detected in roman pot detectors (in other words, there is no pomeron remnant). A way to see exclusive events would be for instance to look for diffractive events in the two jet event sample in the central part of the calorimeter with a a dijet mass above a high enough mass threshold $M_{threshold}$ so that the size of the expected gap is small ($\sqrt{\xi_1 \xi_2} > M_{threshold}/\sqrt{s}$ and $gap\ size \sim \log(1/\xi)$). If some events are found with a much larger rapidity gap, they should be exclusive since the gap is between the jet and the proton and not between the pomeron remnant and the proton.

3.5. Search for exclusive events at the LHC

The search for exclusive events at the LHC can be performed in the same channels as the ones used at the Tevatron. In addition, some other possibilities benefitting from the high luminosity of the LHC appear. One of the cleanest ways to show the existence of exclusive events would be to measure the dilepton and diphoton cross section ratios as a function of the dilepton/diphoton mass [22, 23]. If exclusive events exist, this distribution should show a bump towards high values of the dilepton/diphoton mass since it is possible to produce exclusively diphotons but not dileptons at leading order as we mentionned in the previous paragraph.

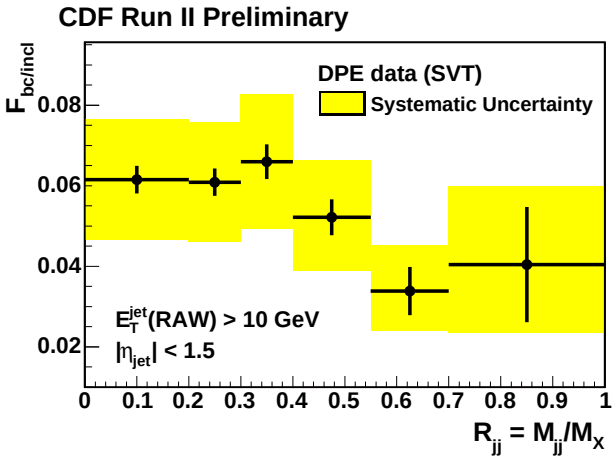

Fig. 11. Ratio of b/c jets to inclusive jets in double pomeron exchange events as a function of the dijet mass fraction.

The search for exclusive events at the LHC will also require a precise analysis and measurement of inclusive diffractive cross sections and in particular the tails at high β since it is a direct background to exclusive event production. It will be also useful to measure directly the exclusive jet production cross section as a function of jet p_T as an example and compare the evolution to the models. This will allow to know precisely the background especially to Higgs searches which we will discuss in the following.

4. Diffraction at the LHC

In this section, we will describe briefly some projects concerning diffraction at the LHC. We will put slightly more emphasis on the diffractive production of heavy objects such as Higgs bosons, top or stop pairs, WW events, etc...

4.1. Diffractive event selection at the LHC

The LHC with a center-of-mass energy of 14 TeV will allow us to access a completely new kinematical domain in diffraction. So far, three experiments, namely ATLAS and CMS-TOTEM have shown interests in diffractive measurements. The diffractive event selection at the LHC will be the same as at the Tevatron. However, the rapidity gap selection will no longer be possible at high luminosity since up to 35 interactions per bunch crossing are expected to occur and soft pile-up events will kill the gaps produced by the hard interaction. Proton tagging will thus be the only possibility to

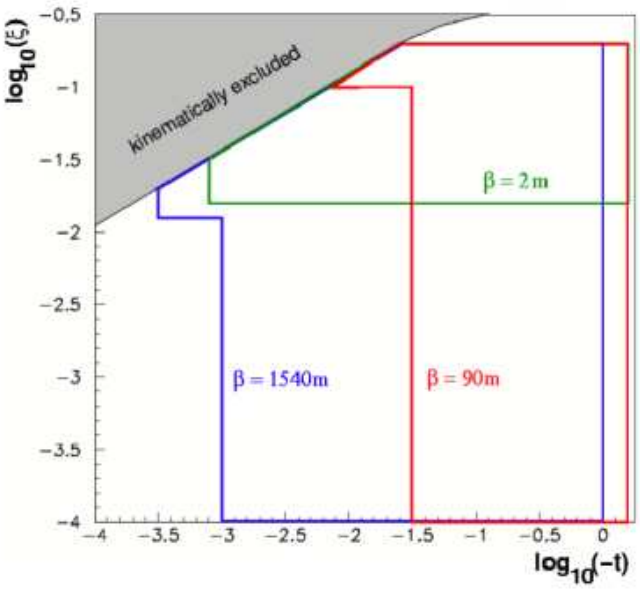

Fig. 12. TOTEM acceptance for different lattices.

detect diffractive events at high luminosity. Let us note that this is not straightforward: we need to make sure that the diffracted protons come from the hard interaction and not from the soft pile up events. The idea we will develop in the following is to measure precisely the time of arrival of the diffracted protons in the forward detectors, and thus know if the protons come from the vertex of the hard interaction.

4.2. Measurements at the LHC using a high β^* lattice in ATLAS-ALFA and TOTEM

Measurements of total cross section and luminosity are foreseen in the ATLAS-ALFA [24] and TOTEM [25] experiments, and roman pots are installed at 147 and 220 m in TOTEM and 240 m in ATLAS. These measurements will require a special injection lattice of the LHC at low luminosity since they require the roman pot detectors to be moved very close to the beam. The acceptance of the TOTEM detectors for different injection lattices is given in Fig. 12, and the possibilities to measure the t-dependence of the total cross section using the different injection lattices in Fig. 13. We notice that high β^* lattices are needed if one wants to access the low-t measurement of the total cross section.

The measurement of the total cross section to be performed by the

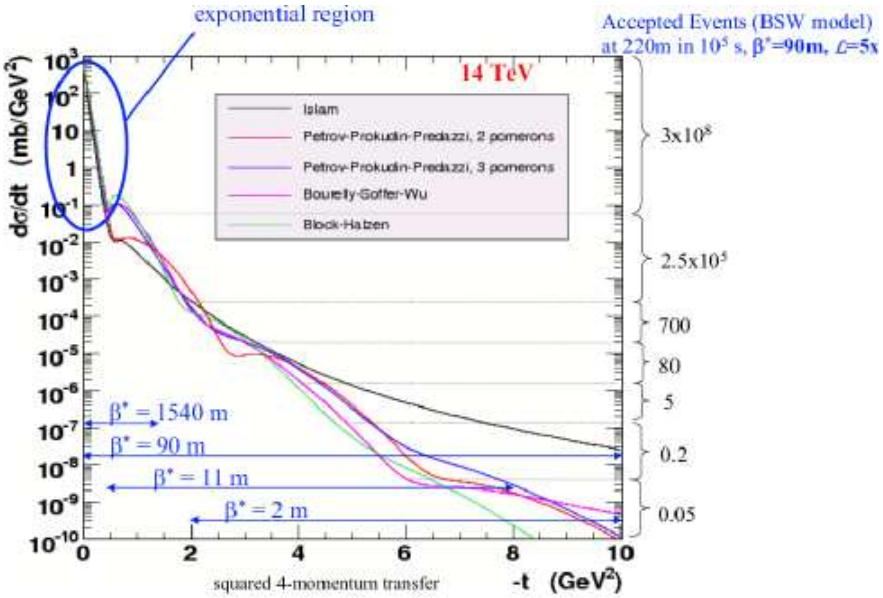

Fig. 13. Measurement of the elastic section and domain accessible for different β^*.

TOTEM collaboration [25] is shown in Fig. 22. We notice that there is a large uncertainty on prediction of the total cross section at the LHC energy in particular due to the discrepancy between the two Tevatron measurements. The inelastic $p\bar{p}$ cross section was measured at a center-of-mass energy of 1.8 TeV at the Tevatron by the E710, E811 and CDF collaborations which lead to the following respective results: 56.6 ± 2.2 mb, 56.5 ± 1.2 mb and 61.7 ± 1.4 mb [26]. While the E710 and E811 experiments agree (E811 is basically the follow up of E710), the E811 and CDF measurements disagree by 9.2%, and the reason is unclear [26]. The measurement of TOTEM will be of special interest to solve that ambiguity as well.

The ATLAS collaboration prefers to measure the elastic scattering in the Coulomb region [24], typically at very low t ($|t| \sim 6.5\ 10^{-4}$ GeV^2). When t is close to 0, the t dependence of the elastic cross section reads:

$$\frac{dN}{dt}(t \to 0) = L\pi \left(\frac{-2\alpha}{|t|} + \frac{\sigma_{tot}}{4\pi}(i+\rho)e^{-b|t|/2} \right)^2 . \tag{3}$$

From a fit to the data in the Coulomb region, it is possible to determine directly the total cross section σ_{tot}, the ρ and b parameters as well as the absolute luminosity L. This measurement requires to go down to $t \sim 6.5\ 10^{-4}$ GeV^2, or $\theta \sim 3.5$ μrad (to reach the kinematical domain where the strong amplitude equals the electromagnetic one). The UA4 collaboration already

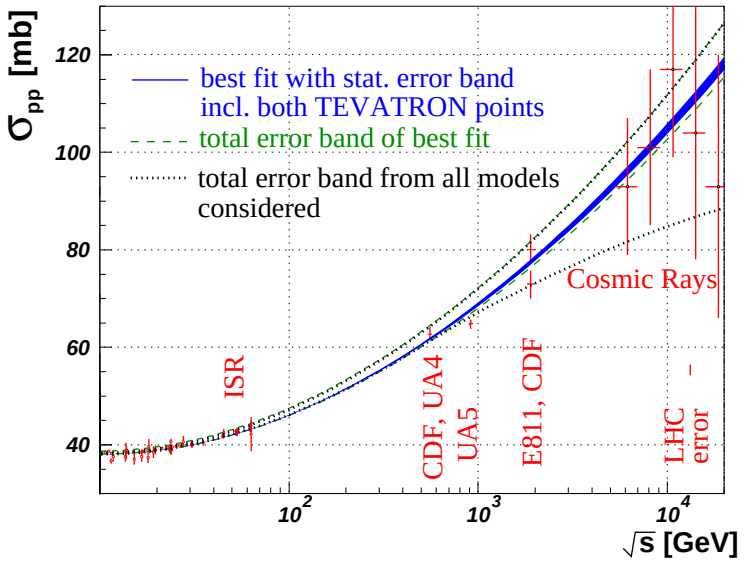

Fig. 14. Measurement of the total cross section.

performed such a measurement at the SPS and reached a precision of the order of 3%. However, the UA4 experiment [27] needed to perform a measurement down to 120 μrad whereas the ATLAS collaboration needs to go down to 3.5 μrad, which is very challenging. This measurement requires a special high β^* lattice, the detectors to be installed 1.5 mm from the LHC beam, a spatial resolution of these detectors well below 100 μm and no significant dead edge on the detector (less than 100 μm).

The solution to perform this measurement is to install two sets of roman pot detectors on each side of ATLAS located at about 240 m from the interaction point, which can go close to the beam when the beam is stable. Each roman pot is itself made of two detectors in the vertical direction. The detector installed in the roman pot is made of 20 $\times$ 64 square 0.5 $\times$ 0.5 mm^2 scintillating fibers on ceramic substrate read out by 24 Multianode photomultipliers with 64 channels. The detector follows a U/V geometry with 45 degree stereo layers, 64 fibers per plane in a module, 10 double sided modules per pot. The up and down detectors overlap for relative alignment purposes.

To check the accuracy of the measurement within ATLAS, a full simulation of elastic events was performed for two values of t: $t = 7.\ 10^{-4}$ GeV^2 and $t = 10^{-5}$ GeV^2. A fit to dN/dt using 10 million events leads to a measurement of luminosity and the total cross section with a statistical precision

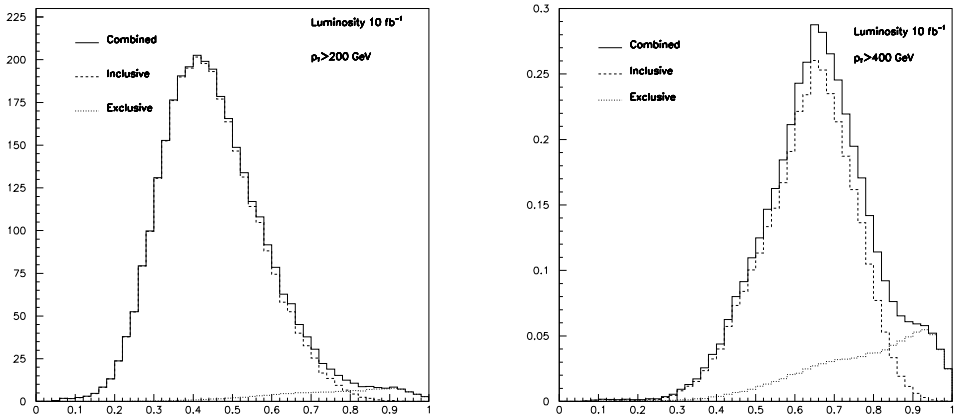

Fig. 15. Dijet mass fraction at the LHC for jets $p_T > 200\,\mathrm{GeV}$ and $p_T > 400\,\mathrm{GeV}$ showing the contribution of both inclusive and exclusive diffraction.

of 1.5% and 0.74% respectively [24].

Once the absolute luminosity and the total cross section are known using these methods, the relative luminosity measurement as a function of time will be performed in ATLAS using the LUCID detector (Luminosity measurement Using Cerenkov Integrating Detectors) [24]. The front face of the LUCID detector is located about 17 meters from the ATLAS interaction point and covers a domain in rapidity of $5.4< |\eta| <6.1$. The principle of the LUCID detector is quite simple. 168 Aluminium tubes are filled with C_4F_{10} or isobutane at 1 or 2 bar pressure. Winston cones at the end of each tube bring the Cerenkov light onto quartz fibers. It is thus possible to measure the number of particles which are produced in the very forward region which is directly related to the instantaneous luminosity. The LUCID detector is mainly sensitive to primary particles only: much more light comes from primary particles than from secondaries or soft particles. The time resolution is about 140 ps which allows to determinate the luminosity bunch by bunch at the LHC. The detector allows to obtain a linear relationship between luminosity and the number of tracks counted in the detector which leads to an easy measurement of luminosity.

4.3. Hard inclusive and exclusive diffraction at the LHC

In this section, we would like to discuss first how we can measure the gluon density in the pomeron, especially at high β since the gluon in this

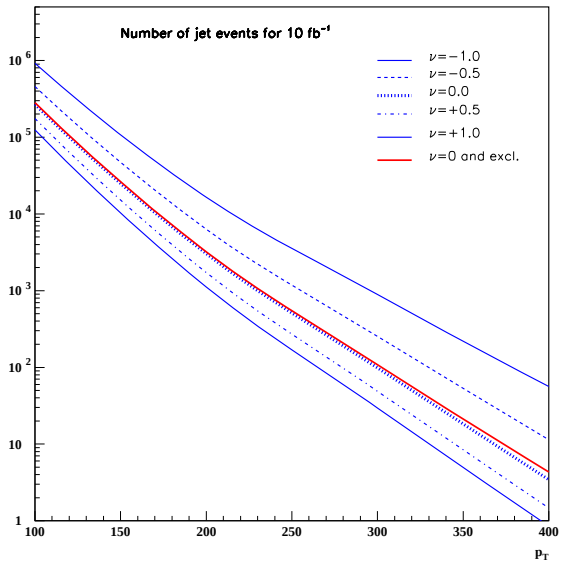

Fig. 16. Number of DPE events at the LHC as a function of minimal transverse momentum p_T^{min} of the two leading jets for different values of the ν parameter (describing the gluon in the pomeron at high β). The effect of adding the exclusive contribution when $\nu = 0$ is also shown and is quite small with respect to the effects of the different ν values.

kinematical domain shows large uncertainties and this is where the exclusive contributions should show up. To take into account the high-β uncertainties of the gluon distribution, we chose to multiply the gluon density in the pomeron measured at HERA by a factor $(1-\beta)^\nu$ where ν varies between -1.0 and 1.0 as we already mentioned in a previous section (see Fig. 9).

The dijet mass fraction as a function of different jet p_T is visible in Fig. 15 after a simulation of the ATLAS/CMS detectors. The exclusive contribution manifests itself as an increase in the tail of the distribution which can be seen for 200 GeV jets (left) and 400 GeV jets (right) respectively [21]. Exclusive production slowly turns on with the increase of the jet p_T which is demonstrated in Fig. 16, where the number of expected double pomeron exchange events for different values of ν with and without the exclusive contribution is shown. However, with respect to the uncertainty on the gluon density this appearance is almost negligible. In that sense, it is possible to use the diffractive dijet cross section measurement as a function

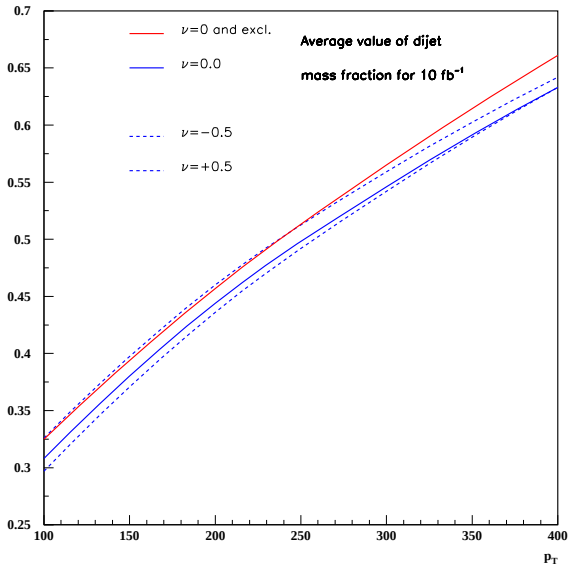

Fig. 17. Average value of the dijet mass fraction as a function of minimal transverse momentum p_T^{min} of the leading jets. Exclusive contribution and different values of ν are shown and its effect is clearly visible, especially for high jet transverse momentum.

of jet transverse momentum to measure more precisely the gluon density in the pomeron at high β. In Fig. 17, we give the average value of the dijet mass fraction for different values of the minimal jet transverse momentum and with and without the exclusive contribution, and we see that exclusive events have the tendency to increase sensibly the average value of the dijet mass fraction. One can use the average position of the dijet mass fraction as a function of the minimal jet transverse momentum p_T^{min} to study the presence of the exclusive contribution, once the gluon density in the pomeron is better known. This is true especially for high p_T jets.

The exclusive production at the LHC plays a minor role for low p_T jets. Therefore, measurements e.g for $p_T < 200\,\mathrm{GeV}$ where the inclusive production is dominant could be used to constrain the gluon density in the pomeron. Afterwards, one can look in the high p_T jet region to extract the exclusive contribution from the tail of the dijet mass fraction.

Other measurements already mentionned such as the diphoton, dilepton cross section ratio as a function of the dijet mass, the b jet, W and Z cross

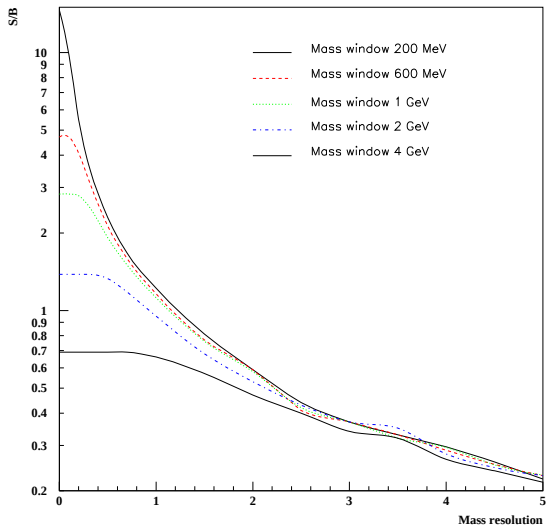

Fig. 18. Standard Model Higgs boson signal to background ratio as a function of the resolution on the missing mass, in GeV. This figure assumes a Higgs boson mass of 120 GeV.

section measurements will be also quite important at the LHC.

4.4. Exclusive Higgs production at the LHC

As we already mentionned in one of the previous sections, one special interest of diffractive events at the LHC is related to the existence of exclusive events and the search for Higgs bosons at low mass in the diffractive mode. So far, two projects are being discussed at the LHC: the installation of roman pot detectors at 220 m in ATLAS [29], and at 420 m for the ATLAS and CMS collaborations [28].

The results discussed in this section rely on the DPEMC Monte Carlo to produce Higgs bosons exclusively [22, 30] and a fast simulation of a typical LHC detector (ATLAS or CMS). Results are given in Fig. 18 for a Higgs mass of 120 GeV, in terms of the signal to background ratio S/B, as a function of the Higgs boson mass resolution. Let us notice that the background is mainly due to the exclusive $b\bar{b}$ production. However the tail of the inclusive $b\bar{b}$ production can also be a relevant contribution and this is related to the high β gluon density which is badly known at present. The expected number of events after all cuts is expected to be of the order of 5

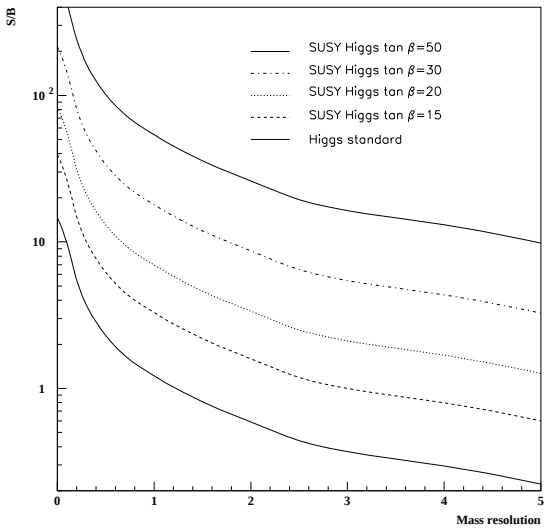

Fig. 19. SUSY Higgs boson signal to background ratio as a function of the resolution on the missing mass, in GeV. This figure assumes a Higgs boson mass of 120 GeV.

for a luminosity of 60 fb^{-1}. In order to obtain a S/B of 1, a mass resolution of about 1.2 GeV is needed which is technically feasible, the inconvenient being the small number of events.

The diffractive SUSY Higgs boson production cross section is noticeably enhanced at high values of $\tan\beta$ and since we look for Higgs decaying into $b\bar{b}$, it is possible to benefit directly from the enhancement of the cross section contrary to the non diffractive case. A signal-over-background up to a factor 50 can be reached for 100 fb^{-1} for $\tan\beta \sim 50$ [31] (see Fig. 19).

More extensive studies including pile up effects and all background sources were performed recently [32] to study in more detail the signal over background for MSSM Higgs production. The ratio R of the number of diffractive Higgs bosons in MSSM to SM are given in Fig. 20. We notice that almost the full plane in ($\tan\beta$, M_A) can be covered (typically if $R >$10, the number of events should be enough to be detected using the diffractive production). In Fig. 21, we give the number of background and MSSM Higgs signal events for a Higgs mass of 120 GeV for $\tan\beta \sim$40. The signal significance is larger than 3.5 σ for 60 fb^{-1} (see Fig. 21 left) and larger than 5 σ after three years of data taking at high luminosity at the LHC and using timing detectors with a resolution of 2 ps (see Fig. 21 right).

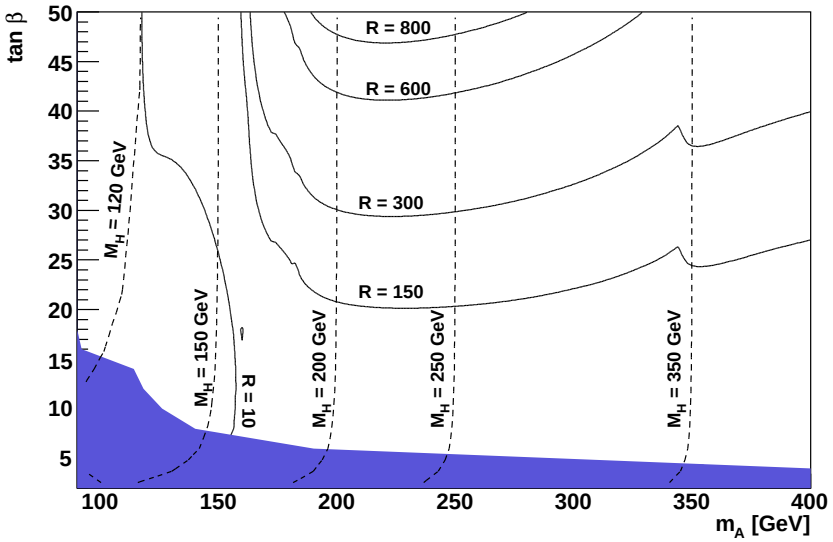

Fig. 20. Ratio R at generator level between the number of diffractive Higgs events in MSSM to SM in the ($\tan\beta$, M_A) plane. The lines of constant Higgs boson mass are also indicated in dashed line.

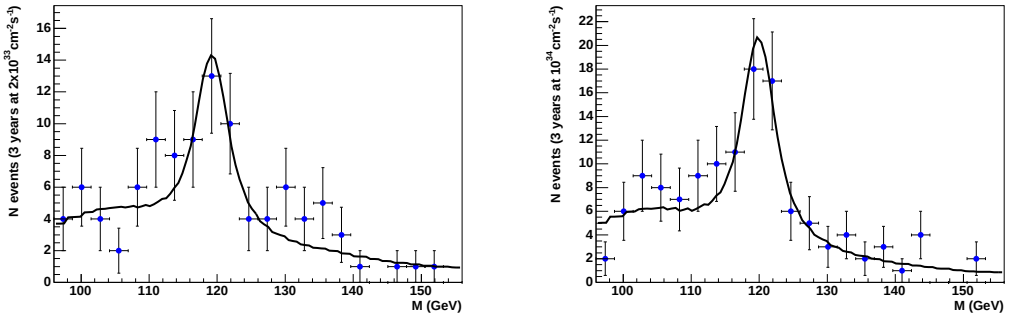

Fig. 21. Higgs signal and background obtained for MSSM Higgs production. The signal significance is larger than 3.5 σ for 60 fb^{-1} (left plot) and larger than 5 σ after three years of data taking at high luminosity at the LHC and using timing detectors with a resolution of 2 ps (right plot).

4.5. Exclusive top, stop and W pair production at the LHC

In the same way that Higgs bosons can be produced exclusively, it is possible to produce W, top and stop quark pairs. WW bosons are produced via QED processes which means that their cross section is well determined. On the contrary, top and stop pair production are obtained via double pomeron exchanges and the production cross section is still uncertain.

The method to reconstruct the mass of heavy objects double diffractively produced at the LHC is based on a fit to the turn-on point of the missing mass distribution at threshold [33].

The threshold scan is directly sensitive to the mass of the diffractively produced object (in the WW case for instance, it is sensitive to twice the WW mass). The idea is thus to fit the turn-on point of the missing mass distribution which leads directly to the mass of the produced object, the WW boson.

The precision of the WW mass measurement (0.3 GeV for 300 fb^{-1}) is not competitive with other methods, but provides a precise check of the calibration of the roman pot detectors. WW events will also allow to assess directly the sensitivity to the photon anomalous coupling since it would reveal itself by a modification of the well-known QED WW production cross section. We can notice that the WW production cross section is proportional to the fourth power of the γW coupling which ensures a very good sensitivity of that process [34]. The precision of the top mass measurement might however be competitive, with an expected precision better than 1 GeV at high luminosity provided that the cross section is high enough. The other application is to use the so-called "threshold-scan method" to measure the stop mass [31]. After taking into account the stop width, we obtain a resolution on the stop mass of 0.4, 0.7 and 4.3 GeV for a stop mass of 174.3, 210 and 393 GeV for a luminosity (divided by the signal efficiency) of 100 fb^{-1} provided that the cross section is high enough.

The caveat is of course that the production via diffractive exclusive processes is model dependent — the production cross section dependence on mass of the produced object depends on the models — and definitely needs the Tevatron and LHC data to test the models. It will allow us to determine more precisely the production cross section by testing and measuring at the Tevatron the jet and photon production for high masses and high dijet or diphoton mass fraction.

5. The AFP and FP420 projects at the LHC

5.1. Motivation

The motivation to install forward detectors at in ATLAS and CMS is quite clear. It extends nicely the project of measuring the total cross sections in ATLAS and TOTEM by measuring hard diffraction at high luminosity at the LHC. Two locations for the forward detectors are considered at 220 and 420 m respectively to ensure a good coverage in ξ or in mass of the diffractively produced object as we will see in the following. Installing forward detectors at 420 m is quite challenging since the detectors will be located in the cold region of the LHC and the cryostat has to be modified to accomodate the detectors. In addition, the space available is quite small and some special mechanism called movable beam pipe are used to move the detectors close to the beam when the beam is stable enough. The situation at 220 m is easier since it is located in the warm region of the LHC and both roman pot and movable beam pipe technics can be used. The AFP (ATLAS Forward Physics) project is under discussion in the ATLAS collaboration and includes both 220 and 420 m detectors on both sides of the main ATLAS detector.

The physics motivation of this project corresponds to different domains of diffraction which we already discussed in these lectures:

- A better understanding of the inclusive diffraction mechanism at the LHC by studying in detail the structure of pomeron in terms of quarks and gluons as it was done at HERA [6, 12]. Of great importance is also the measurement of the exclusive production of diffractive events [21] and its cross section in the jet channel as a function of jet transverse momentum. Its understanding is necessary to control the background to Higgs signal.

- Looking for Higgs boson diffractive production in double pomeron exchange in the Standard Model or supersymmetric extensions of the Standard Model [22, 31]. This is clearly a challenging topic especially at low Higgs boson masses where the Higgs boson decays in $b\bar{b}$ and the standard non-diffractive search is difficult. We will detail in the following the trigger strategy.

- Sensitivity to the anomalous coupling of the photon by measuring the QED production cross section of W boson pairs [34]. This is one of the best ways to access the anomalous coupling before the start of the ILC. Photoproduction of jets can also be studied. %
- Other topics such as looking for stop events or measuring the top mass using the threshold scan method [33] which will depend strongly on the production cross section.

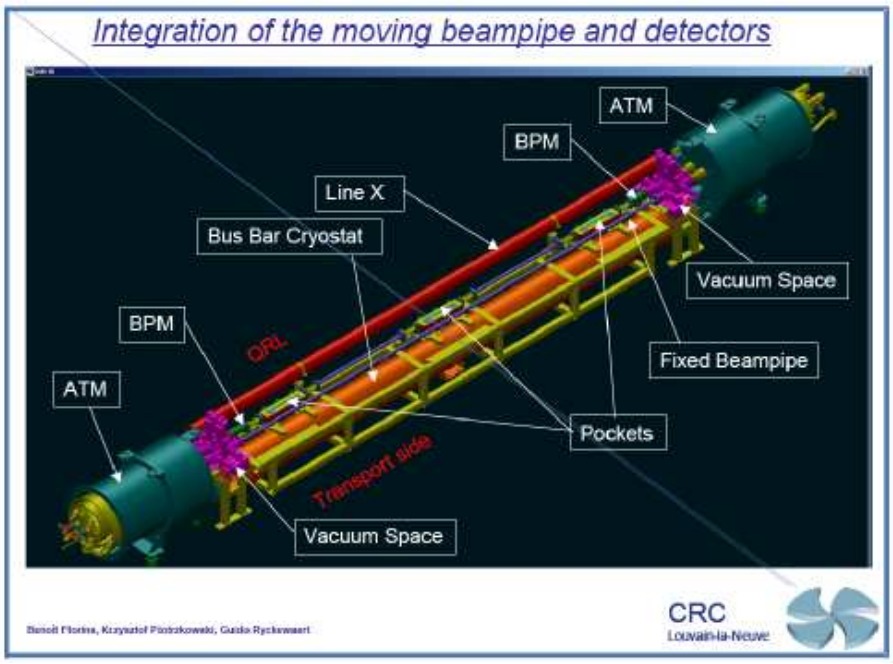

Fig. 22. Scheme of the movable beam pipe.

5.2. Forward detector design and location

As we mentionned in the previous section, it is needed to install movable beam pipe detectors [28, 29] at 420 m. The scheme of the movable beam pipe is given in Fig. 22. The principle developed originally for the ZEUS detector to tag electrons at low angle is quite simple and follows from the same ideas as the roman pots. The beam pipe is larger than the usual one and can host the sensitive detectors to tag the diffracted protons in the final state. When the beam is stable, the beam pipe can move so that the detectors can be closer to the beam. The movable beam pipe acts in a way as a single direction roman pot. In Fig. 22, we see the Beam Position Monitors (BPM) as well as the pockets where the detectors can be put. The detectors can be aligned and calibrated using the BPMs as well as exclusive dimuon events.The dimuon mass can be well measured using the central muon detectors from ATLAS and can be compared to the result obtained using the missing mass method by tagging the final state proton in the forward detectors. This allows to calibrate the forward detectors by using data directly. The exclusive muon production cross section is expected to be high enough to allow this calibration on a store-by-store basis.

The AFP project proposes to install in addition some forward detectors in ATLAS at about 220 m on each side of the main ATLAS detector [29]. A few options are still under discussion and we will discuss only the favoured option at present. The first component is the same as at 420 m, namely the movable beam pipe containing the pockets where both the horizontal Si and timing detectors can be located. However, it is not possible to use exclusive dimuon events for calibration purposes at 220 m since the cross section is too small (the acceptance of 220 m detectors is better for high mass objects, and so higher dimuon masses, which leads to a smaller production cross section). For calibration and alignment, the idea is to use BPMs as before and also elastic events. The acceptance in elastic events in the horizontal detectors in the movable beam pipe is however very small, and this is why the idea is to use additional detectors (vertical roman pots) for calibration purposes. The vertical roman pots can be aligned using the ξ distribution pointing at 0 for elastics, and the horizontal detectors in the movable beam pipe can be calibrated with respect to the vertical detectors using common events in both detectors (halo or single diffractive events). With this method, some preliminary studies show that a precision up to 5 μm on calibration using elastics is within reach. The roman pot design follows as close as possible the design which is currently used by the TOTEM collaboration and the Luminosity group of the ATLAS collaboration. Another design would be to have only the timing detectors in the movable beam pipes and three-arm roman pots holding the horizontal and vertical 3D Si detectors.

The missing mass acceptance is given in Fig. 23. The missing mass acceptance using only the 220 m pots starts at 135 GeV, but increases slowly as a function of missing mass. It is clear that one needs both detectors at 220 and 420 m to obtain a good acceptance on a wide range of masses since most events are asymmetric (one tag at 220 m and another one at 420 m). The precision on mass reconstruction using either two tags at 220 m or one tag at 220 m and another one at 420 m is of the order of 2-4 % on the full mass range, whereas it goes down to 1% for symmetric 420 m tags.

5.3. Detectors inside forward detectors for the AFP project

We propose to put inside the forward detectors two kinds of detectors, namely 3D Silicon detectors to measure precisely the position of the diffracted protons, and the mass of the produced object and ξ, and precise timing detectors.

The position detectors will consist in 3D Silicon detector which allow to obtain a resolution in position better than 10 μm. The detector is made of 10 layers of 3D Si pixels of 50 $\times$ 400 μm. One layer contains 9 pairs of columns of 160 pixels, the total size being 7.2 $\times$ 8 mm^2. The detectors will

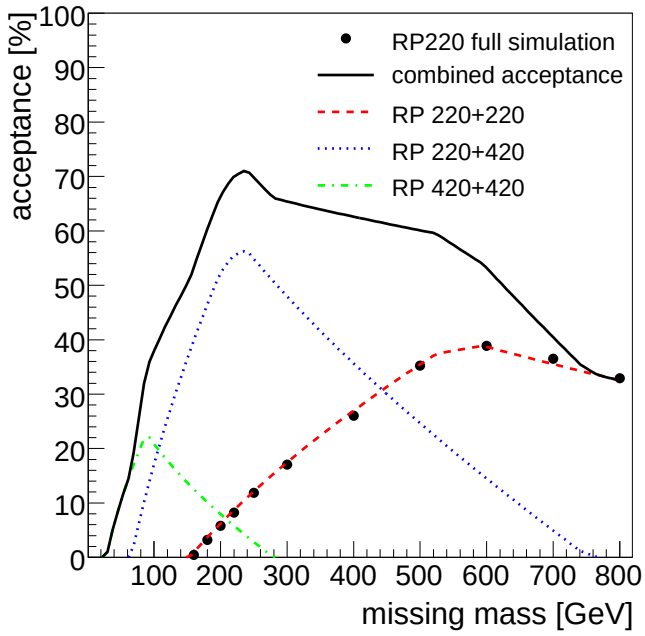

Fig. 23. Roman pot detector acceptance as a function of missing mass assuming a 10σ operating positions, a dead edge for the detector of 50 μm and a thin window of 200 μm.

be read out by the standard ATLAS pixel chip [28, 29]. The latency time of the chip is larger than 6 μs which gives enough time to send back the local L1 decision from the roman pots to ATLAS (see the next paragraph about trigger for more detail), and to receive the L1 decision from ATLAS, which means a distance of about 440 m. It is also foressen to perform a slight modification of the chip to include the trigger possibilities into the chip. It is planed to install the roman pot together with the Silicon detectors during a shut down of the LHC in 2010.

The timing detectors are necessary at the highest luminosity of the LHC to identify from which vertex the protons are coming from. It is expected that up to 35 interactions occur at the same bunch crossing and we need to identify from which interaction, or from which vertex the protons are coming from. A precision of the order of 1 mm or 2-5 ps is required to distinguish between the different vertices and to make sure that the diffracted protons come from the hard interactions. Picosecond timing detectors are still a challenge and are developped for medical and particle physics applications.

Two technogies are developped, either using as a radiator — with the aim to emit photons by the diffracted protons —- gas(gas Cerenkov detector or GASTOF) or a crystal of about 2.5 cm (QUARTIC), and the signal can be read out by Micro-Channel Plates Photomultipliers developped by Photonis [28, 29]. The space resolution of those detectors should be of the order of a few mm since at most two protons will be detected in those detectors for one given bunch crossing at the highest luminosity. The detectors can be read out with a Constant Fraction Discriminator which allows to improve the timing resolution significantly compared to usual electronics. A first version of the timing detectors is expected to be ready in 2010 with a resolution of 20-30 ps, and the final version by 2012-2013 with a resolution of 2-5 ps.

5.4. Trigger principle and rate

In this section, we would like to give the principle of the trigger using the roman pots at 220 m as well as the rates obtained using a simulation of the ATLAS detector and trigger framework [29].

The principle of the trigger is shown in Fig. 24 in the case of a Higgs boson decaying into $b\bar{b}$ as an example. The first level trigger comes directly from two different 3D Silicon layers in each forward detector. It is more practical to use two dedicated planes for triggering only since it allows to use different signal thresholds for trigger and readout. The idea is to send at most five strip addresses which are hit at level 1 (to simplify the trigger procedure, we group all pixels in vertical lines as one element only for the trigger since it is enough to know the distance in the horizontal direction to have a good approximation of ξ). A local trigger is defined at the roman pot level on each side of the ATLAS experiment by combining the two trigger planes in each roman pot and the roman pots as well. If the hits are found to be compatible (not issued by noise but by real protons), the strip addresses are sent to ATLAS, which allows to compute the ξ of each proton, and the diffractive mass. This information is then combined with the information coming from the central ATLAS detector, requesting for instance two jets above 40 GeV in the case shown in Fig. 24. At L2, the information coming from the timing detectors for each diffracted proton can be used and combined with the position of the main vertex of ATLAS to check for compatibility. Once a positive ATLAS trigger decision is taken (even without any diffracted proton), the readout informations coming from the roman pot detectors are sent to ATLAS as any subdetector.

The different trigger possibilities for the roman pots are given below:

- **Trigger on DPE events at 220 m:** This is the easiest situation since two protons can be requested at Level 1 at 220 m. Three different

options are considered:
- *trigger on high mass Higgs* ($M > 160$ GeV) given by ATLAS directly (decay in WW, ZZ),
- *inclusive trigger on high mass object* by requesting two high p_T jets and two positive tags in roman pots,
- *trigger on jets* (high p_T jets given directly by ATLAS, and low p_T jet special trigger for QCD studies highly prescaled).
This configuration will not rise any problem concerning the L1 rate since most of the events will be triggered by ATLAS anyway, and the special diffractive triggers will be for QCD measurements and can be highly prescaled.

- **Trigger on DPE events at 220 and 420 m:** This is the most delicate scenario since the information from the 420 m pots cannot be included at L1 because of the L1 latency time of ATLAS. The strategy is the following (see Table 1):
- *trigger on heavy objects* (Higgs...) decaying in $b\bar{b}$ by requesting a positive tag (one side only) at 220 m with $\xi < 0.05$ (due to the 420m RP acceptance in ξ, the proton momentum fractional loss in the 220m roman pot cannot be too high if the Higgs mass is smaller than 140 GeV), and topological cuts on jets such as the exclusiveness of the process $((E_{jet1} + E_{jet2})/E_{calo} > 0.9$, $(\eta_1 + \eta_2) \cdot \eta_{220} > 0$, where $\eta_{1,2}$ are the pseudorapidities of the two L1 jets, and η_{220} the pseudorapidity of the proton in the 220m roman pots). This trigger can hold without prescales to a luminosity up to 2.10^{33} cm^{-2}s^{-1},
- *trigger on jets* (single diffraction, or double pomeron exchange) for QCD studies: can be heavily prescaled,
- *trigger on W, top...* given by ATLAS with lepton triggers.
Let us note that the rate will be of the order of a few Hz at L2 by adding a cut on a presence of a tag in the 420 pots, on timing, and also on the compatibility of the rapidity of the central object computed using the jets or the protons in roman pots.

6. Conclusion

In these lectures, we presented and discussed the most recent results on inclusive diffraction from the Tevatron experiments and gave the prospects for the future at the LHC. Of special interest is the exclusive production of Higgs boson and heavy objects (W, top, stop pairs) which will require a better understanding of diffractive events and the link between ep and hadronic colliders, and precise measurements and analyses of inclusive diffraction at the LHC in particular to constrain further the gluon density in the pomeron.

$\mathcal{L}$ $E_T > 40\,\text{GeV}$	n_{pp} per bunch crossing	2-jet rate [kHz] $[\text{cm}^{-2} \cdot \text{s}^{-1}]$	RP200 reduction factor	$\xi < 0.05$ reduction factor	Jet Prop.
1×10^{32}	0.35	2.6	120	300	1200
1×10^{33}	3.5	26	8.9	22	88
2×10^{33}	7	52	4.2	9.8	39.2
5×10^{33}	17.5	130	1.9	3.9	15.6
1×10^{34}	35	260	1.3	2.2	8.8

Table 1. L1 rates for 2-jet trigger with $E_T > 40\,\text{GeV}$ and additional reduction factors due to the requirement of triggering on diffractive proton at 220 m, and also on jet properties.

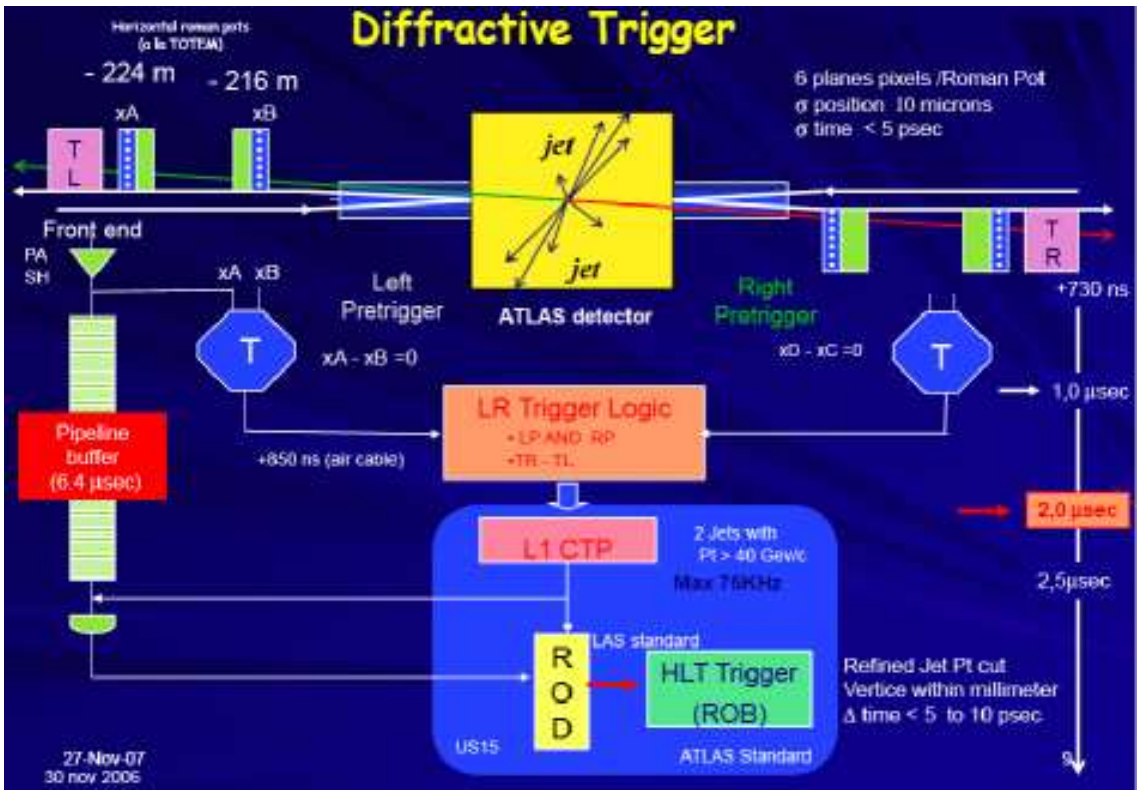

Fig. 24. Scheme for L1 trigger for the AFP project.

The search for exclusive events at the Tevatron is quite promising especially in the dijet channel. We finished the lectures by describing the main projects

to install forward detectors at the LHC, and especially the AFP project to measure diffraction at high luminosity.

Acknowledgments

I thank Robi Peschanski for a careful reading of the manuscript.

REFERENCES

[1] B. Loehr, contribution about "Diffraction at HERA" at this Summer school

[2] M. Rangel, C. Royon, G. Alves, J. Barreto, R. Peschanski, Nucl. Phys. B**774** (2007) 53; M. Rangel these proceedings.

[3] CDF Collaboration, Phys. Rev. Lett. **87** (2001) 241802; Phys. Rev. Lett. **78** (1997) 2698; D0 Collaboration Phys. Lett. **B574** (2003) 169; Phys. Lett. **B 531** (2002) 52.

[4] See http://www-cdf.fnal.gov and http://rock23.rockefeller.edu/.

[5] Proposal for a Forward Proton Detector at DØ , DØ Collaboration (1997), Proposal P-900 to FERMILAB PAC.

[6] H1 Collaboration, Eur. Phys.J. C**48** (2006) 715; H1 Collaboration, Eur. Phys.J. C**48** (2006) 749; H1 Collaboration, Z. Phys. C**76** (1997) 613; ZEUS Collaboration, Nucl. Phys. B**713** (2005) 3.

[7] J.Bartels, J.Ellis, H.Kowalski, M.Wuesthoff, Eur.Phys.J.C7 (1999) 443, J.Bartels, C.Royon, Mod. Phys. Lett. **A14** (1999) 1583.

[8] A.H.Mueller and B.Patel, Nucl. Phys. **B425** (1994) 471; A.H.Mueller, Nucl. Phys. **B437** (1995) 107; A.H.Mueller, Nucl. Phys. **B415** (1994) 373; H.Navelet, R.Peschanski, Ch.Royon, S.Wallon, Phys. Lett. **B385** (1996) 357; A. Bialas, R.Peschanski, C.Royon, Phys. Rev. **D57** (1998) 6899; S.Munier, R.Peschanski, C.Royon, Nucl. Phys. **B534** (1998) 297; M. Boonekamp, A. De Roeck, C. Royon, S. Wallon, Nucl. Phys. **B555** (1999) 540.

[9] K. Golec-Biernat and M. Wusthoff, Phys. Rev. **D59** (1999) 014017; Phys. Rev. **D60** (1999) 114023.

[10] G.Altarelli and G.Parisi, *Nucl. Phys.* **B126** 18C (1977) 298; V.N.Gribov and L.N.Lipatov, *Sov. Journ. Nucl. Phys.* (1972) 438 and 675; Yu.L.Dokshitzer, *Sov. Phys. JETP.* **46** (1977) 641.

[11] G. Ingelman, P.E. Schlein, Phys. Lett. **B152** (1985) 256.

[12] C. Royon, L. Schoeffel, J. Bartels, H. Jung, R. Peschanski, Phys. Rev. **D63** (2001) 074004; C. Royon, L. Schoeffel, R. Peschanski, E. Sauvan, Nucl. Phys. B**746** (2006) 15; C. Royon, L. Schoeffel, S. Sapeta, R. Peschanski, E. Sauvan, Nucl. Phys. B**781** (2007) 1.

[13] J. Collins, Phys. Rev. D**57** (1998) 3051.

[14] M. Gallinaro, talk given at the DIS 2006 workshop, 20-24 April 2006, Tsukuba, Japan, see /http://www-conf.kek.jp/dis06/; Dino Goulianos, talk given at

the low x 2006 workshop, June 28 - July 1 2206, Lisbon, Portugal, see http://www-d0.fnal.gov∼royon/lowx_lisbon; CDF Collaboration, Phys. Rev. Lett. **88** (2002) 151802.

[15] CDF Collaboration, Phys. Rev. Lett. **84** (2000) 5043; Phys. Rev. Lett. **87** (2001) 141802.

[16] A. Kupčo, R. Peschanski, C.Royon, Phys. Lett. **B606** (2005) 139, and references therein.

[17] A. Edin, G. Ingelman, J. Rathsman, Phys. Lett. B**366** (1996) 371.

[18] CDF Collaboration, analysis and results described in: http://www-cdf.fnal.gov/physics/new/qcd/abstracts/dpe_ex_07.html.

[19] CDF Collaboration, Phys. Rev. Lett. 99 (2007) 242002.

[20] CDF Collaboration, preprint hep-ex/0712.0604.

[21] O.Kepka, C. Royon, Phys. Rev.D**76** (2007) 034012; O. Kepka, C. Royon these proceedings.

[22] C. Royon, Mod. Phys. Lett. A **18**, 2169 (2003) and references therein; M. Boonekamp, R. Peschanski, C. Royon, Phys. Rev. Lett. **87** (2001) 251806; Nucl. Phys. **B669** (2003) 277; M. Boonekamp, A. De Roeck, R. Peschanski, C. Royon, Phys. Lett. **B550** (2002) 93; V.A. Khoze, A.D. Martin, M.G. Ryskin, Eur. Phys. J. **C19** (2001) 477; Eur. Phys. J. **C23** (2002) 311; Eur. Phys. J. **C24** (2002) 581; arXiv:0802.0177; Phys. Lett. B650 (2007) 41; A.B. Kaidalov, V.A. Khoze, A.D. Martin, M.G. Ryskin, Eur. Phys. J. **C33** (2004) 261; Eur. Phys. J. **C31** (2003) 387

[23] C. Royon, preprint Fermilab-CONF-06-018E, hep-ph/0601226; TeV4LHC QCD Working Group, FERMILAB-CONF-06-359, hep-ph/0610012.

[24] ATLAS Coll., see http://atlas-project-lumi-fphys.web.cern.ch/atlas-project-lumi-fphys/; C. Royon, Proccedings of Science DIFF2006 (2006) 021.

[25] TOTEM Coll., see http://totem.web.cern.ch/Totem/, TOTEM Technical Design Report,

[26] E710 Collaboration, Phys. Rev. Lett. **63** (1989) 2784; E811 Collaboration, Phys. Lett. B**445** (1999) 419; CDF Collaboration, Phys. Rev. D**50** (1994) 5550.

[27] UA4 Coll., Phys. Lett. B**198** (1987) 583.

[28] FP420 Coll., see http://www.fp420.com

[29] AFP TDR in ATLAS to be submitted; see: http://project-rp220.web.cern.ch/project-rp220/index.html; C. Royon, preprint arXiv:0706.1796, proceedings of 15th International Workshop on Deep-Inelastic Scattering and Related Subjects (DIS2007), Munich, Germany, 16-20 Apr 2007.

[30] See http://boonekam.home.cern.ch/boonekam/dpemc.htm

[31] M. Boonekamp, J. Cammin, S. Lavignac, R. Peschanski, C. Royon, Phys. Rev. **D73** (2006) 115011, and references therein.

[32] B. Cox, F. Loebinger, A. Pilkington, JHEP 0710 (2007) 090; S. Heinemeyer et al., Eur. Phys. J. C **53** (2008) 231.

[33] M. Boonekamp, J. Cammin, R. Peschanski, C. Royon, Phys. Lett. B**654** (2007) 104.

[34] O. Kepka, C. Royon in preparation.